Markus Hempel

Programming and Evaluation of an Ultra-Wideband Distance Measurement System for Mobile Robots

INF FAKULTÄT FÜR INFORMATIK

Intelligent Cooperative Systems
Computational Intelligence

Programming and Evaluation of an Ultra-Wideband Distance Measurement System for Mobile Robots

Bachelor Thesis

Markus Hempel

January 22, 2019

Supervisor: Prof. Dr.-Ing. habil. Sanaz Mostaghim

Advisor: Dr.-Ing. Christoph Steup

Advisor: Sebastian Mai, M.Sc.

Markus Hempel: *Programming and Evaluation of an Ultra-Wideband Distance Measurement System for Mobile Robots*
Otto-von-Guericke Universität
Intelligent Cooperative Systems
Computational Intelligence
Magdeburg, 2019.

Abstract

To enable positioning in areas without GPS, alternative localization methods must be used. Here multilateration with ultra wideband(UWB) distance measurements can be applied. This thesis discusses the implementation and evaluation of single UWB distance measurements for the use with mobile robots. Disturbances occurring during the measurements, such as multipath effects, frequency interferences and the movement of the robot, are discussed and experiments are designed to investigate these. After a suitable implementation of a double-sided two way ranging algorithm with DecaWave DWM1000 modules, the error over distance as well as the influence of disturbances were analyzed by the experiments. Results show, that distance measurements with UWB are feasible. However disturbances influence the yielded distances and limit the applicability, especially if multiple disturbances cumulate.

Contents

List of Figures

List of Tables

List of Listings

1 Introduction

Today the use of mobile robots is rapidly increasing. Whether in today's economy as logistic robots used in warehouses, or as agile drones with multiple purposes from the delivery of packages to usage in photography or the military. Many tasks get carried out by robots of any form and type.[9] In this thesis a distance measurement system with ultra wideband was chosen and evaluated in regard to disturbances and applicability with mobile robots.

1.1 Motivation

The use of drones is of special interest. The FINken project, run by the faculty of computer science at the Otto-von-Guericke University Magdeburg, aims to create a swarm of autonomous quadcopters. Most of the time the copters fly in a copter arena of 4x3 meters inside the swarm laboratory. The maximal distance, that can be measured in this arena, is 5 meters in diagonal. A single copter has a diameter of approximately 30 centimeters. To fly a swarm of copters within the arena, fast and precise position information are needed to prevent a collision between them.

It is possible to determine these positions with the help of the global positioning system(GPS) [10]. But inside of buildings, like warehouses, it is not possible to receive satellite signals for a correct GPS position.
Because of that, a good indoor positioning solution is needed.

A robot position can be calculated in several ways. By combining multiple distances (multilateration), angles (multiangulation) or time differences [46], measured from different sources, a position can be computed. Due to the combined use of multiple measurements, a resulting positioning error can be partly minimized.

In this thesis especially multilateration is of concern, because the used hardware only supports the measurement of distances. Despite the error is partly

minimized by multilateration, still good single distance measurements are needed to compute an accurate position. Those single distance measurements are further called ranging.

Of particular interest here is the time of flight ranging with ultra wideband radio waves.
Goal of this thesis is to implement a suitable ranging algorithm for a ranging with ultra wideband. The quality and applicability of this ranging is evaluated through conducted experiments.

In order to use ranging and to carry out a quality assessment, criteria must be found against which the quality can be measured. From these criteria, requirements for good ranging can be derived.

1.2 Requirements for Ranging

For the evaluation of ranging methods it is necessary to define criteria for a good ranging. Here concrete comparable criteria for quality of a ranging are found. On the basis of these criteria important ranging requirements can be defined and a suitable evaluation of the ranging can be carried out. Thus a good ranging can be classified.
Furthermore including the above mentioned quality criteria different ranging approaches can be compared among each other in terms of applicability, which is further described in section 2.

Requirements for the ranging can be differentiated between requirements for the specific values yielded by the ranging, further called hard requirements, and requirements regarding the approach itself and its feasibility, further called soft requirements.

Hard requirements

A good ranging approach should yield distances of useful quality. Here the mean error μ of the measurement, calculated as the difference between the

measured distance values by the system and the actual distances obtained by a reference system, is used. It can be expressed as equation 1.1, where N is the total number of measurements, $\hat{d}$ is the measured distance and d is the real distance. [12]

$$\mu = \frac{\sum_1^N |\hat{d} - d|}{N} \tag{1.1}$$

Further the standard deviation σ of the mean error is used to analyze a ranging. It is expressed as the degree of mutual agreement among a series of individual measurements. The standard deviation is calculated by equation 1.2. [12]

$$\sigma = \sqrt{\frac{\sum_1^N (\hat{d} - \mu)^2}{N}} \tag{1.2}$$

When the mean error and the standard deviation are low, the ranging and therefore computed robot location contains minimal errors. With mean error values under 30 centimeters and a standard deviation under 15 centimeters a ranging should be feasible, depending on the application scenario. To fly the quadcopter swarm in the arena scenario, these are the minimum required values.

Distances of a good ranging also need to be updated in short intervals, so the time without available positions can be minimized. This improves the performance of the mobile robot and enables the use of the ranging even on fast moving robots like drones.

A fulfillment of the above mentioned requirements secure an exact ranging with minimal errors and enable robots to work mostly unsupervised.

Soft requirements

To support multiple use cases, a ranging solution is needed that works independent of its location, whether at outdoor or indoor locations.
The maximal usable distance of the ranging should fit the location and the use case with mobile robots.

Furthermore, there are external error sources, that can influence the ranging. Therefore a low susceptibility to external error sources, like multipath effects at obstacles and frequency interferences, is a requirement for a robust ranging.

The ranging approach itself should not interfere with the robots performance. That means a robot should be able to include the physical devices for range measurements and thus enable an easy installation on a wide range of applications.
A modular software implementation for easier integration in existing software systems supports the use in more applications as well.

In order to evaluate the feasibility of ranging with ultra wideband, in the next chapter different approaches are compared based on the above stated requirements. The comparison results in ultra wideband time of flight as the best approach. Therefore the used hardware is further described and a suitable implementation of a ranging is carried out. The quality of this ranging is then evaluated through experiments. The tests show, that ultra wideband time of flight is applicable for an indoor use. However the use of ultra wideband is associated with accuracy variations and is therefore subject to restrictions.

2 State of the Art

2.1 Existing Ranging Solutions

Keeping the earlier mentioned requirements for ranging from section 1.2 in mind, there are other suitable technologies for ranging.
Most of the applications using ranging technologies rely on positioning instead of pure ranging. By combining multiple measurements to calculate a position, errors in single measurements can be partly emended. So it is difficult to compare pure ranging applications and positioning applications.
However many of these positioning applications use multilateration to calculate positions. Only range measurements are combinedly utilized to calculate the positions like in pure ranging. This enables a certain comparability between different solutions in terms of suitability for the use with mobile robots. Based on the comparison can be decided on the possible use and further analysis of the respective solution.

	RSSI	Phase Shift	Ultrasonic	UWB-TOF	Optical	UWB-TDOA
Accuracy	--	+	+	++	++	+
Update Freq.	++	++	--	++	++	++
max. Distance	--	+	+	++	-	+
Robustness	--	+	-	+	-	-
Integration	++	+	+	+	--	--
Price	++	++	++	++	--	+

Table 2.1: Comparison of approaches

Table 2.1 shows the comparison between different approaches. Here, the approaches are compared in terms of the previously established requirements and additionally the purchase price of the individual components. If possible, accuracy is the combination of mean error and standard deviation of the yielded result values. Robustness is the susceptibility to environmental noise and integration summarizes the construction and possible implementation of

the solution. Ultra wideband time of flight achieves the best results in overall comparison.

The analysis of every approach is described in the following sections. Afterwards a detailed comparison is given.

2.1.1 Ranging based on Signal Strength

A property of radio waves, which can be used for ranging, is signal strength. The further the source of the signal is away the weaker the signal gets. This property can be used to build a ranging based on Received Signal Strength Indication(RSSI).
Bluetooth, WLAN and RFID [39, 31, 28, 22] are technologies, which enable RSSI-based ranging, so already existing technologies can be reused RSSI-transceivers lie within an affordable price range of under 50 dollar [1], are small and hence easy to integrate in applications.

However there are several problems with RSSI-based ranging. The attenuation rate is the rate α at which the signal strength decreases over distance:

$$SignalStrength \propto Distance^{\alpha}.$$

As a rule of thumb, if $\alpha = 2$ then signal strength drops by 3 decibel every time distance doubles. This sub-linear attenuation rate means that the difference in signal strength between 1m and 2m is similar to the difference between 10m and 20m. A constant level of noise can therefore result in an ever increasing error, when signal strength is used to estimate distance. As shown in figure 2.1, changes in signal strength due to distance become small relative to noise, even if the level of noise remains the same over distance [45].

Additionally there are severe multipath effects by radio wave reflections from walls and obstacles during indoor use. Furthermore, through the build characteristics of transceivers the antennas never propagate radio waves with equal signal strength in every direction from the source [21].
The transceiver will be mounted on robots containing mainly metallic materials, which can block radio signals. Based on the orientation of the robot and the transceiver the signal strength varies a lot.
The above mentioned characteristics lead to a small usable range with bad accuracy and robustness.

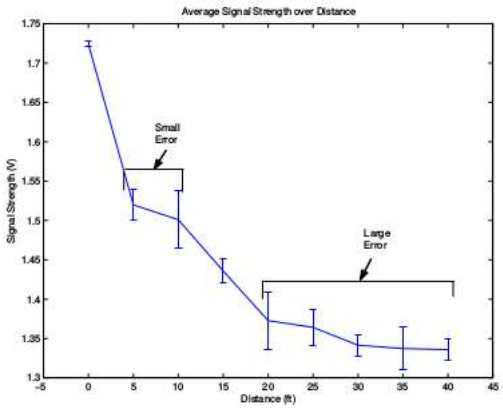

Figure 2.1: RSSI - Error increase over distance [45]

2.1.2 Ranging based on Phase Differences

Another property of radio signals, that can be utilized for ranging, is phase shift.
By sending out radio signals of different frequencies the reflected signals from the target can be compared with the sent ones. Between these signals, phase differences can be observed. A resulting distance can be computed out of these phase differences [38].

The property of phase shift can be used to get accurate to high accurate result values, as well as reasonable ranging distances. An implementation of ranging with phase differences by Qiu [40] yields values shown in figure 2.2.

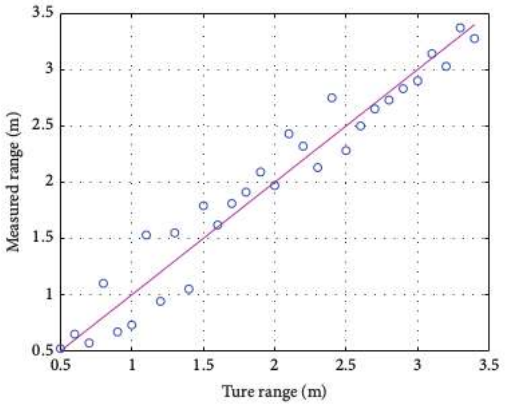

Figure 2.2: Yielded values with phase difference ranging [40]

With this implementation a mean error of 10 to 20 centimeters can be achieved.
The range measurements were repeated several times for different tag angles. Here, range measurements show a tag angle insensitivity [40].
This is especially useful for use with mobile robots.

By using radio signals to measure the phase shift a high update frequency is given. Also small and affordable radio frequency transceivers [1] can be used, which enable an easy integration.

However ranging inaccuracy can be caused by multipath effects, frequency interferences in the environment or variations over temperature [40].

2.1.3 Ultrasonic Time of Flight

Other ranging approaches, like Cricket and Active Bat [33], use sound to calculate a distance. By measuring the time between the sent sound signal and the related reflection of that signal (echo) a distance can be computed with equation 2.1, where v_{sound} is the velocity of sound and t_{round} is the measured round trip time. [41]

$$Distance = v_{sound} \cdot \frac{t_{round}}{2} \tag{2.1}$$

Sound signals propagate much slower than radio signals. This enables an easier measurement of the time of flight, but also limits the update frequency of distance values [15]. Especially for ranging on longer distances or when multiple robots want to range to each other, the slower propagation time sets an upper limit to the performance. To calculate distances between a swarm of 5 robots, the upper boundary of the update frequency is 5 Hz [32]. So the performance on fast moving robots is drastically limited.

The ranging accuracy in this approach is prone to decrease due to changes in temperature, air humidity and atmospheric pressure, because they interfere with the physical properties of sound propagation.

Ultrasonic range finders are purchasable at an affordable price of under 50 $ [5]. They are small and because of that easy to integrate in a variety of applications.

Ultrasonic ranging is typically used for obstacle detection, instead of ranging, in submarines as well as in automotive applications or to control liquid levels in industrial tanks [3].

2.1.4 Ultra Wideband Time of Flight

A distance can be measured by calculating the time of flight of radio signals between a sender and a receiver. Because bandwidths over 500 MHz are used to communicate in, it is called ultra wideband.
Here, time stamped messages are used to communicate between sender and receiver. With these time stamps a time of flight, hence an adequate distance, can be computed by multiplication with the speed of light as shown in equation 2.2. Here, d is the resulting distance, T_{prop} is the time of flight and c_{air} is the speed of light in the medium air. The speed of light in air equals 299700 kilometers per second [6].

$$d = c_{air} \cdot T_{prop} \tag{2.2}$$

Michler et al. [35] states, that in reflectionless environments, as well as in typical multipath environments, an error deviation better than three centimeters and a mean error better than three millimeters can be reached.
In free space scenarios, ranges of up to 280 meters could be achieved while still keeping the system's accuracy at a high level.
Influential here is the use of ultra wideband, because a larger bandwidth will increase the robustness against frequency interferers and multipath propagation [35].
Experiments by Cardinali et al. [14] support Michler's statements as their results showed, that the presence of multipath effects strongly affects ranging accuracy but favors a larger bandwidth [14].

By using radio signals to measure the phase shift a high update frequency can be achieved. The DWM1000 modules are small and affordable radio frequency transceivers [2], which enable an easy integration.

2.2 Existing Positioning Solutions

Existing solutions don't rely only on ranging distances to compute a position. Solutions, that compute their position not relying on single distance measurements are described below. The earlier mentioned requirements are applied on the quality of the resulting position instead of the ranging.

2.2.1 Optical Tracking

A solution used in many applications is optical tracking. Cameras of visible or infrared light range are used to observe the tracked device. Optical tracking relies, like human vision, on the principle of stereopsis, which is a type of multiangulation, to calculate distances.
Targets can be tracked with the help of markers placed on the target or, if the camera is integrated in the target, as stationary markers around the target. The camera tracks these markers and calculates distances to them [34].
After a successful calibration the optical tracking system yields highly accurate values with jitter under 1 mm and has a high update frequency.
Here, jitter is the mean error, and thus the deviation of the measured distance from the real distance. It is therefore correlated to the accuracy of the solution.

Applied to our scenario, the use with mobile robots, problems with this solution can be found in the difficult calibration of the cameras. A further problem is the small maximal usable range, because the jitter in values increases with distance to the object.

In figure 2.3 the correlation of distance to the camera and the corresponding quadratic increase in jitter can be seen. Here, multiple cameras for optical tracking are compared regarding their jitter with distances up to 2.5 meters. For a 1 m Flashpoint camera the jitter at 1 meter is about 0.02 millimeters, but at 2 meters the jitter is already about 0.08 millimeters.

With coefficients a, b, c for each camera the jitter can be estimated with formula 2.3, where z is the distance to the camera in meters [29].

$$J(z) = \frac{az^2 + bz + c}{10000} \tag{2.3}$$

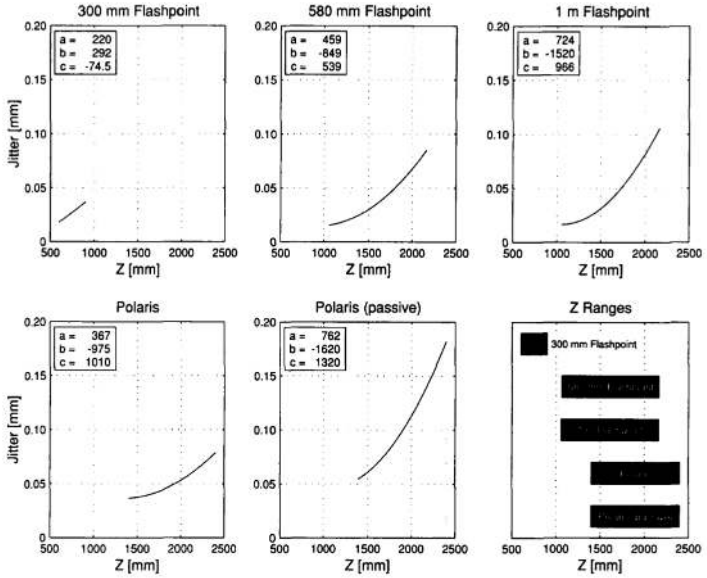

Figure 2.3: Jitter-Distance-Correlation [29]

Optical tracking is less susceptible to noise from the environment, but is in need of a direct line of sight to a marker to calculate a correct distance. So obstacles interrupting the line of sight and concealing the tracked object would have an impact on the usability of this solution up to the point where no distance can be measured.
This solution is also limited by the view angle of the camera. So measurements to an object outside the view angle can not be carried out. Furthermore optical tracking requires the integration of multiple cameras. Therefore expensive equipment (OptiTrack cameras 279$ [4]) is required and integrated in the application.

2.2.2 Ultra Wideband Time Difference of Arrival

The position of a device can be determined using time difference of arrival (TDOA) information based on radio frequency signal arrival-time measurements. No absolute times are used to determine a distance, instead distances get computed out of time differences. No reference to a common clock between sender and receiver is needed.

TDOA utilizes multilateration to calculate a location. Here two approaches are common: the "surveillance" approach and the "navigation" approach.

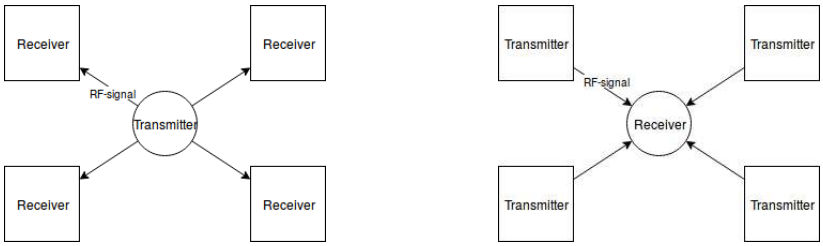

(a) Surveillance (b) Navigation

Figure 2.4: TDOA Approaches

"Surveillance" approach

A transmitter can be located with the help of multiple receivers as shown in figure 2.4. The radio frequency pulses emitted by the transmitter will arrive at different times at the receivers due to different distances to them. The time of arrival is measured and out of these values the time difference of arrival at each receiver is calculated. Therefore the location and the absolute clocks of the receivers must be known. Out of the time differences the location of the transmitter can be estimated by forming hyperbolas of same time differences. The hyperbola intersections are the estimated locations of the transmitter. The doppler frequency shift can be used to determine the speed and heading of the transmitter as well.
By adding more receivers the accuracy of the calculated location can be increased and errors can be minimized.

"Navigation" approach

A receiver can locate itself with the help of multiple transmitters as shown in figure 2.4. Here, the signals emitted from the transmitters get received, the time of arrival of each signal is stored and time differences are calculated. The differences are then multiplied with the propagation of the signals and so distances can be multilaterally computed. This only applies if the locations of the transmitters are known and all signals are sent at the exact same time on different frequencies to avoid interference. Otherwise actions, like broadcasting with a specific delay for every transmitter or embedding an unique known code to the signal, are necessary to differentiate between the transmitters.

Limitations

Both approaches need a minimum of n+1 stations (whether receiver or transmitter) to locate a single device, where n is the dimension of the localization area. This leads to the use of 4 stations in a 3D localization environment. All of the used stations need to be interconnected and synchronized in time, which is a large cost factor. To get the distance to one single device at least 2 stations are needed. Else the relative measured time of arrival can not be set in absolute context by comparing it to another time of arrival measurement. Also for best results the stations should surround the application area. The integration in an application use case therefore requires time and effort.

Because radio frequency pulses are transmitted, the yielded solution is prone to attenuation through objects, phase cancellation and multipath effects, which can render the estimation rather inaccurate. Furthermore to get an accurate location unique multilateral intersections of at least three measurements need to be calculated by solving non linear equations, which requires high computational costs. In noisy environments it is rather difficult to find unique intersections. Therefore no exact location can be computed, instead an area of possible locations is found. [24, 27, 25, 20]

2.3 Comparison Result

As shown in table 2.1 ultra wideband time of flight achieves the best results in overall comparison.
A RSSI-based ranging will yield less useful results in terms of accuracy and robustness and is not a feasible approach for the use with mobile robots.
Because of the characteristics, the use of ranging based on phase differences is not feasible in an area with many obstacles or with a crowded frequency band. If that is not the case, this approach is only inferior to ultra wideband time of flight in terms of accuracy and maximal distance and is suitable.
Ultrasonic time of flight can be used for single distance measurements, but for using it with multiple robots the update frequency limitations, due to a slower propagation velocity, are to severe for this approach to be practicable.
Because precise and accurate values are yielded by an optical tracking, this seems to be an suitable approach for ranging. But the drawbacks in integration, robustness and maximal distance render this solution rather

unfeasible. Optical tracking can still be used in obstacle free environments at small to medium ranges. Because it is less susceptible to environmental noise, the use in areas with high external influences is possible. Furthermore optical tracking can be used to set a baseline for other methods.
Ultra wideband time difference of arrival has drawbacks in integration of this solution as well as in accuracy. Additionally the noise susceptibility renders this approach not feasible for the use in applications.
Ultra wideband time of flight ranging seems to be the most accurate and robust approach. Thus it is most feasible for a high dynamic environment like mobile robots.

Therefore ranging modules, like the ones used by Michler et al.[35], were integrated in a ranging application and further analyzed over the course of this thesis. In the following chapter the characteristics of the used modules are described.

3 DWM-Module Characteristics

In this thesis, DWM1000 modules were used. A DWM1000 module "is a fully integrated low-power, single chip CMOS RF transceiver IC compliant with the IEEE 802.15.4-2011 UWB standard"[17]. An antenna and all associated analog and radio frequency components are integrated in the DWM1000-Module. The mounted module is shown in figure 3.1.
It was soldered to a custom printed circuit board and communicates with a STM32-L443 microcontroller.

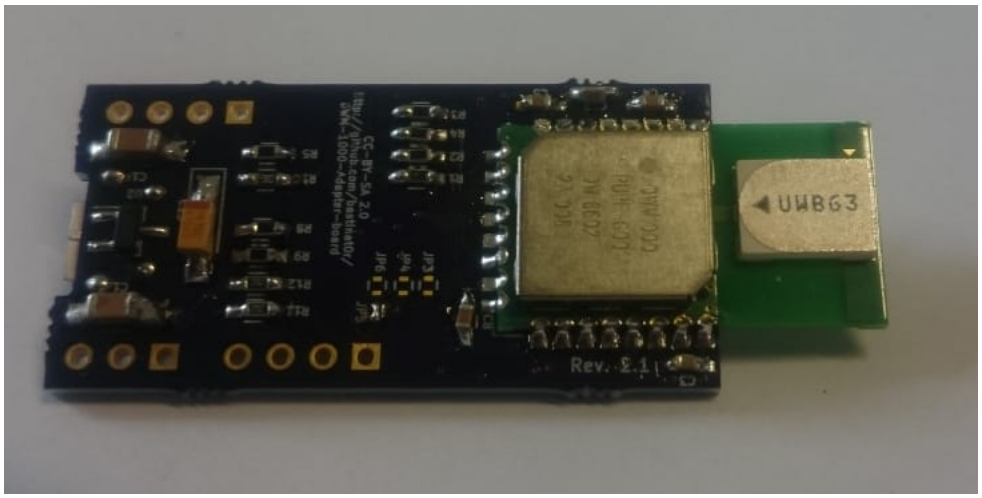

Figure 3.1: Mounted DWM-Module

3.1 Antenna Characteristics

The DWM-Module uses ultra-wideband signals to measure distances. Hereby radio signals are send between the modules. This allows to calculate the time-of-flight from one module to another and so an adequate distance.

By using radio signals, variances in signal strength can occur depending on how the DWM-Module itself is constructed and mounted on the application board. The radio waves transmitted by a module can be blocked by the application board. The mounting on the range to object can block the transmission as well, but this is application-dependant.

As shown in the module schematic in figure 3.2, the integrated antenna is constructed as an external part of the module offside the application board. These construction properties serve the purpose of enabling a signal transmission free from interference.

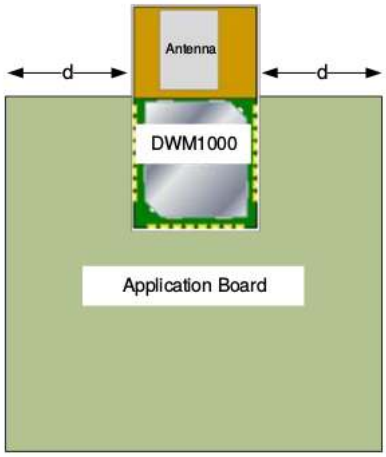

Figure 3.2: Schematic DWM-Module
[19]

Even though a blocking-free transmission is achieved, the transmission power varies through the construction of the antenna itself. In figure 3.3, the different antenna radiation patterns on 3 different planes are shown[19].
"As the antenna is linearly polarised, in the Azimuth plane the vertically polarised field (Theta) is measured and the horizontally polarised field (Phi) is measured for elevation planes 1 and 2"[19].
This means the azimuth plane can be seen as the propagation direction of the electromagnetic wave, where as for theta and phi the perpendicular electric field and the magnetic field vectors are measured [37]. The measured signal strength in these planes differs with the deviation to the propagation

direction of the wave. On each plane, the measurements forming the antenna radiation plot were conducted on two transmit channels 2 and 5 with different bandwidths to compensate for errors by frequency interference.

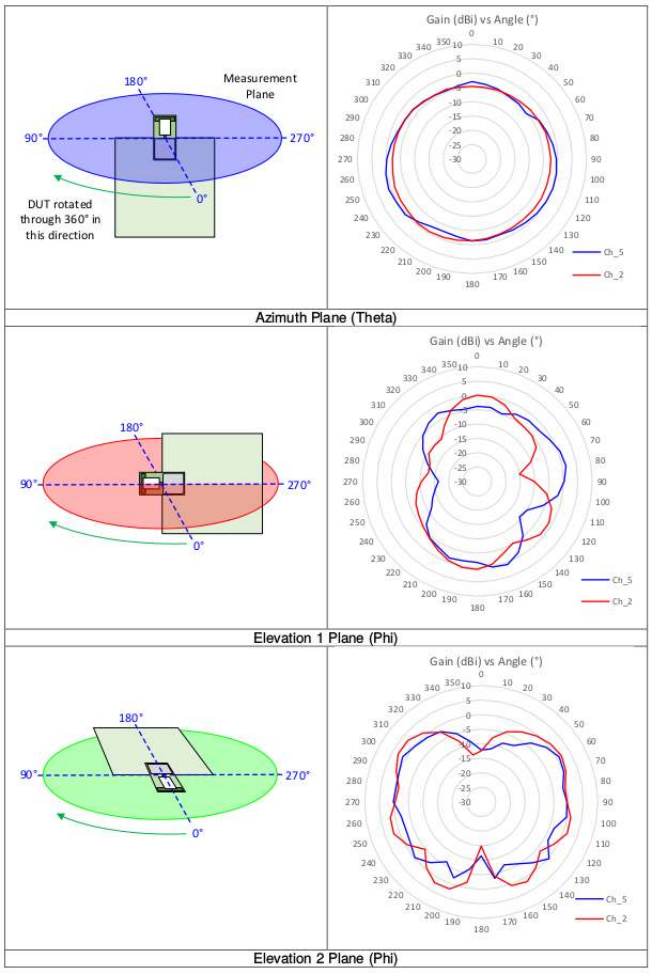

Figure 3.3: Antenna Radiation Patterns
[19]

3.2 Bandwidths Characteristics

The DWM-module can utilize one out of six freely selectable channels, each with an unique bandwidth and center frequency [17]. The center frequency is

the arithmetic mean between the upper and lower frequency boundaries of the channel. So the upper and lower boundaries can be computed with equation 3.1.

$$boundaryFrequency = centerFrequency \pm \frac{bandwidth}{2} \tag{3.1}$$

Table 3.1 shows the available channels.
The module is able to work in an interval from 3 GHz to 7.5 GHz. The channel must be chosen beforehand and defines the frequency band, that will be used to transceive in. Every module needs to select the same channel to establish a ranging.
Due to the possible use of multiple center frequencies and bandwidths, a flexible application can be created, which is able to adapt and overcome possible limitations due to frequency interferences.

Channel number	Centre frequency (MHz)	Bandwidth (MHz)
1	3494.4	499.2
2	3993.6	499.2
3	4492.8	499.2
4	3993.6	1331.2
5	6489.6	499.2
7	6489.6	1081.6

Table 3.1: Channels and Bandwidths
[17]

3.3 Transmit parameters

Flexible usage in all kinds of applications can be achieved by adjusting up to 3 additional transmit parameters. The transmitted data rate, the pulse frequency and the length of the sent preamble can be changed.

As for data rate one out of 3 values, 110 Kbps(kilobit per second), 850 Kbps and 6800 Kbps, can be chosen. Combined with a pulse frequency value of 16

or 64 MHz and a preamble length of 64 to 4096 symbols in steps of powers of two, different transmit modes can be achieved.
Adjustments in data rate influence the maximal transmit range, transmit speed as well as error robustness. The length of the transmitted data and the maximal transmit range can be adjusted through preamble length and the pulse frequency mainly influences the power consumption of the module while ranging.
By adjusting the parameters, the ranging can be adapted to different given circumstances.

3.4 Connection Characteristics

"The DW1000 host communications interface is a slave-only Serial Peripheral Interface (SPI) compliant with the industry protocol. The host system must include a master SPI bus controller in order to communicate with the DW1000. The host system reads and writes DW1000 registers via the SPI."[17] The STM443 microcontroller as host system establishes a SPI connection and controls the module via the corresponding registers.

Due to the characteristics of the modules and the ranging, several disturbances influencing the measurement values yielded by the ranging are unavoidable. In the following chapter possible disturbances are classified and described in detail.

4 Disturbances

Disturbances, that influence the ranging, lead to errors in the yielded measurement values. These measurement errors can be divided into two categories: random error and systematic error.
In the following sections, the sources of systematic and random errors during ranging are described in more detail.

4.1 Systematic Error

Systematic errors of ranging are caused by the ranging module itself. Zug et al. [48] distinguished mainly between constant, continuous and non-continuous internal sensor errors.
Constant errors represent a constant offset from the correct value. Continuous errors can be modeled through multiplicative combination of constant factors to the observed physical values.
As they are identified these types of errors can usually be corrected.
More difficult to detect and correct are non-continuous systematic errors. Here, a case-by-case analysis must be conducted to identify the error, because a simple relation to the true values can not always be found [48].

4.1.1 Applied systematic error

They can be caused by a wrong calibration of the sensor, malfunctioning electronic components or a wrong implementation by the developer [48].

An inaccurate system clock can lead to variances at time stamping of received or transmitted messages. The DWM1000 modules used in this thesis have a worst case clock error of 20 parts per million(ppm) [17]. The reply times are

calculated using time stamps influenced by the clock offset. So the yielded distances get influenced. To compensate for errors resulting from the clock an appropriate ranging algorithm, which minimizes the occurring error, must be found.

The analysis of ranging methods in terms of defectiveness by clock error and applicability is further treated in section 5.5.

4.2 Random Error

Random error is always present in a measurement. It is caused by unpredictable fluctuations in the measurement. These fluctuations may be caused by interference of the environment with the ranging process. Random errors are recognizable as different results for the same repeated measurement. They can mostly be determined by comparing multiple measurements, and reduced by averaging those measurements [43].
Zug et al. [48] classify these types of errors as varying non continuous faults. They are usually caused by the physical properties of the measurement process and get influenced through varying environmental conditions. [48] The random error contains various environment factors that influence the ranging, like multipath effects, frequency interferences, module temperature as well as the changing module orientation due to movement of the robots.

4.2.1 Multipath

Radio signals can not pass through metallic materials and get significant slower traveling through other mediums than air. If an object is in line of sight between two ranging modules, radio waves can not propagate at the direct signal path. So an extended signal path, whether reflected or refracted, will be used. This results in an extended propagation time and therefore in inaccurate distances. [30]
To analyze the impact of multipath effects experiments were carried out and evaluated in section 6.3.

4.2.2 Frequency interferences

The ranging modules can transmit radio signals at a frequency of 3 GHz to 7.5 GHz. Other radio signals in this bandwidth can affect the ranging results due to possible destructive and constructive interferences [42]. Especially the WIFI 5.0 channel bandwidth is encapsuled in this frequency bandwidth. Using this WIFI channel while ranging can influence the yielded results [47]. The impact of the used transmit frequency is evaluated with the help of an experiment in section 6.2.

4.2.3 Ranging in Motion

Robots in real world scenarios are mostly agile. The ranging modules are moving and the positions of the modules related to each other are constantly changing. Based on the module characteristics, referred to in section 3.1, changes in the module orientation lead to influences on the yielded ranging results. Further several experiments were conducted in section 6.4 to evaluate these influences.

4.2.4 Module temperature

While operating the ranging modules heat up. For each degree the output transmit power increases by 0.05 dB [18]. Also the electrical resistance inside the module increases. This can lead to inaccurate range measurements.
Carried out experiments consider no heat increase of the modules, because in practical usage on moving robots this seems to be a less important issue. The modules slowly heat up over an extended time period of constant usage. Therefore an air stream due to movement is cooling the module well enough to prevent these effects from happening. Especially in a quadcopter scenario, the air stream, created by the quadcopter rotors, cools the modules very well. Particularly problems can occur, if the module is situated in a casing and no air stream can cool the module.

To compensate for systematic and module orientation errors as well as to minimize the resulting measurement error an appropriate ranging implementation

must be performed. The influence of other disturbances is evaluated by experiments utilizing the implementation of ranging described in the next chapter.

5 Implementation

The general component structure used in this thesis is shown in figure 5.1. To communicate between a PC and the STM32-L443 microcontroller a connection over UART was established. A SPI connection then links the microcontroller with the DWM1000 module and grants access to it. The establishment of a connection to the module is further treated in section 5.1.
To ensure good measured values, the implementation of the module itself in terms of configuration and orientation is described in sections 5.2 and 5.3.
Then section 5.4 explains the IEEE standard used by the modules to communicate with other modules. Based on the IEEE standard, an appropriate algorithm is chosen to implement a functional ranging between modules in section 5.5.

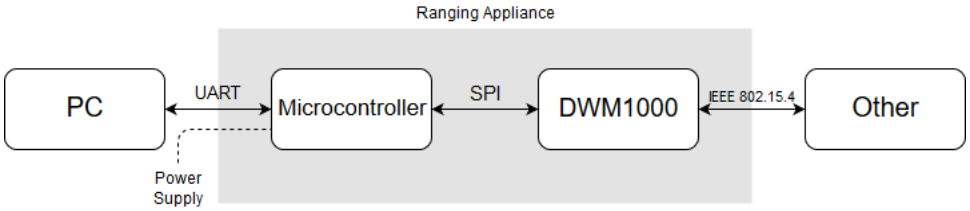

Figure 5.1: Overview Compound Structure

5.1 Interconnection

To program the modules and exchange measurement values, first a connection from a PC to the microcontroller was established using mbed-os with the arm-gcc toolchain. The power supply of the microcontroller is ensured through the connection with the PC. Stand-alone microcontrollers can also be powered by other power sources. Now a communication with the STM32-L443 microcontroller was established.

The microcontroller hosts the used program code and sends commands over an established slave-only SPI connection to the module. In order to access the module functionality in an easy way, the libdw1000 library [11] from bitcraze is used. To program the modules, register values in the modules need to be set bitwise. This can be done with the help of the library, because all basic command functionality is accessible through library functions and the registers are specified through constants.

The used library is written in C and mbed-os utilizes C++, thus the used programming language is C++ to enable a compatibility between the library and mbed-os.

5.2 Module Configuration

As described in chapter 3, the modules have adjustable transmit parameters. The modules used in this thesis were configured with a data rate of 6800 kbps, a pulse frequency of 64 MHz and a preamble length of 128 symbols. This enables the fast transmission of short data between the modules in small to medium distances. It is suited for indoor use and especially for the use with a swarm of quadcopters in the copter arena.
Because the modules have a stable electrical supply by the PC or another power source, power consumption is not of concern here.

5.3 Module Orientation

The angle to the module antenna is directly related to the received signal strength. Worst case values are achieved, if the angle is in the phi and theta plane of the module antenna, because these planes consist of orthogonal in phase components of the propagated electromagnetic wave[37]. Best measurement values can be achieved by transmitting in the propagation direction of the wave. The modules were arranged to perform in the azimuth plane, except for one experiment with changing module orientation. Therefore the angle of the modules to each other had no impact on the yielded result values.

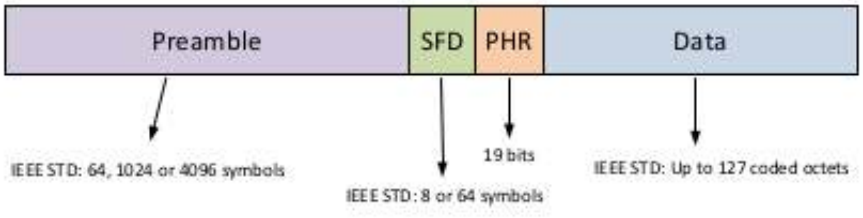

Figure 5.2: Physical Layer Frame Structure[17]

5.4 Module Communication

The ultra wideband communication is based on the transmission and reception of frames.
The UWB physical layer, as specified in the IEEE 802.15.4 - 2011 standard [7], is implemented by the ultra wideband transceivers. Figure 5.2 shows the general structure of a frame.

A frame begins with a synchronisation header consisting of the preamble and the SFD (start of frame delimiter). After that, the PHY header (PHR) defines the length (and data rate) of the data payload part of the frame.

The UWB used in 802.15.4[7] is sometimes called impulse radio UWB because it is based on high speed pulses of radio frequency(RF) energy.

The Synchronisation Header (SHR) consists of the preamble sequence and the SFD (start of frame delimiter).
The synchronisation header is made up of single pulses. The sequence of pulses actually sent during the symbol interval is determined by preamble code. The IEEE 802.15.4 standard[7] defines 8 different length-31 preamble codes for use at 16 MHz pulse repetition frequency and 16 different length-127 preamble codes for use at 64 MHz pulse repetition frequency. The preamble length is defined by how many times (i.e. for how many symbols) the sequence is repeated. This is determined by the configuration of preamble symbol repetitions(PSR). The standard[7] defines PSR settings of 16, 64, 1024 and 4096. The DWM1000 supports these settings. Moreover, it supports PSR settings of 128, 256, 512, 1536 and 2048.

The SFD marks the end of the preamble and the precise start of the PHY Header. The standard specifies the SFD, which consists of the preamble sym-

MAC Header (MHR)							MAC Payload	MAC Footer (MFR)
Frame Control	Sequence Number	Destination PAN Identifier	Destination Address	Source PAN Identifier	Source Address	Aux Security Header	Frame Payload	FCS
2 octets	1 octet	0 or 2 octets	0, 2 or 8 octets	0 or 2 octets	0, 2 or 8 octets	0, 5, 6 10 or 14 octets	Variable number of octets	2 octets

Figure 5.3: General MAC message format [17]

bols. It contains not sent, sent or inverted sent(i.e. 0, +1 or -1) radio frequency pulses in a defined pattern. This pattern is 8 symbols long for data rates other than 110 kbps, and 64 symbols long for the 110 kbps mode.

Forward error correction is included in the PHR and Data parts of the frame. The 19-bit PHR includes a 6-bit single-error-correct double-error-detect (SECDED) code and the data part of the frame has a Reed Solomon (RS) code applied. Both SECDED and RS codes are systematic meaning that the data can be recovered without using the codes.

The DWM1000 fills in the Data Rate, Frame Length, Ranging Packet, and Preamble Duration fields of the PHR based on the user configuration of the appropriate parameters in the register files and generates the SECDED sequence accordingly.

The data part of the UWB frame is occupied by a MAC message specified in the MAC layer defined in the IEEE 802.15.4 - 2011 standard [7]. The general structure of a MAC message consists of a header, that identifies the frame and indicates what components are incorporated in the remainder of the MAC header, followed by a variable length payload typically from the upper layers, and finally ended by the MAC footer which is the frame checking sequence CRC (Cyclic Redundancy Check) used to detect transmission errors [17]. Figure 5.3 shows the general MAC message format.

5.5 Ranging Algorithm

One ranging module functions as the anchor, that initiates the ranging, calculates and yields the resulting distance values. The other module functions as the beacon to which a distance is measured.

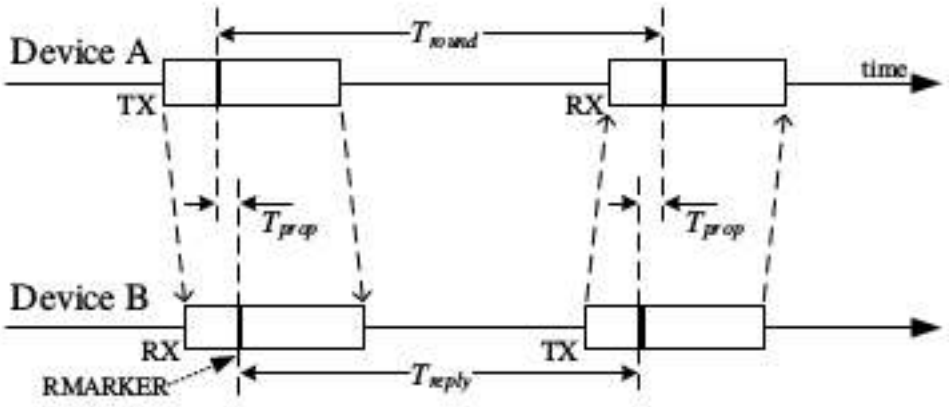

Figure 5.4: Single Sided Two Way Ranging [17]

The ranging is based on transmission and reception of ultra-wideband signals, called frames in further explanation. Every time a frame is communicated, whether received or transmitted, a time stamp is created on the affected module. Out of the created time stamps, reply times and round trip times can be calculated. And out of these values, the resulting time-of-flight is computed.

There are more than one possible algorithms for calculating the time-of-flight between the modules. But which algorithm is best suited for reasonable ranging?

Single Sided Two Way Ranging

A simpler approach is the single sided two way ranging(SSTWR) algorithm. Here one frame exchange between the anchor and beacon happens. So the round and the reply time get calculated separately on each module with its respective local clock. This can be seen in figure 5.4.

The resulting propagation time here can be calculated using equation 5.1 [17].

$$T_{prop} = 0.5 \cdot (T_{round} - T_{reply}) \tag{5.1}$$

However both clocks have a defined clock offset error e (see section 4.1), that gets propagated to a considerable error in the time-of-flight.
The resulting error in the SSTWR is given through equation 5.2 [17].

clock error / T_{reply}	2 ppm	5 ppm	10 ppm	20 ppm	40 ppm
100 µs	0.1 ns	0.25 ns	0.5 ns	1 ns	2 ns
200 µs	0.2 ns	0.5 ns	1 ns	2 ns	4 ns
500 µs	0.5 ns	1.25 ns	2.5 ns	5 ns	10 ns
1 ms	1 ns	2.5 ns	5 ns	10 ns	20 ns
2 ms	2 ns	5 ns	10 ns	20 ns	40 ns
5 ms	5 ns	12.5 ns	25 ns	50 ns	100 ns

Figure 5.5: Typical clock induced errors [17]

$$error = 0.5 \cdot (e_B - e_A) \cdot T_{reply} \tag{5.2}$$

"It can be seen that as T_{reply} increases and as the clock offset increases the error in the time-of-flight estimation increases to the point where the error is such as to render the estimation very inaccurate" [17].
In figure 5.5 the resulting error for selected module reply times and clock errors is shown. An error of one nanosecond is equivalent to an error of 30 centimeters in distance. Even with a low clock error and a small reply time of for example 5 ppm and 500 microseconds the resulting error in distance is 37.5 centimeters, which renders a measurement very inaccurate.

For this reason the SSTWR can only be used for specific use cases with low clock error and minimized reply time. This renders the single sided algorithm unsuitable for a flexible and robust ranging.

Double Sided Two Way Ranging

A better approach is the double sided two way ranging(DSTWR) algorithm. It "is an extension of the basic single-sided two-way ranging in which two round trip time measurements are used and combined to give a time-of-flight result which has a reduced error even for quite long response delays" [17]. This is shown in figure 5.6.

The propagation time can be calculated using equation 5.3 [17].

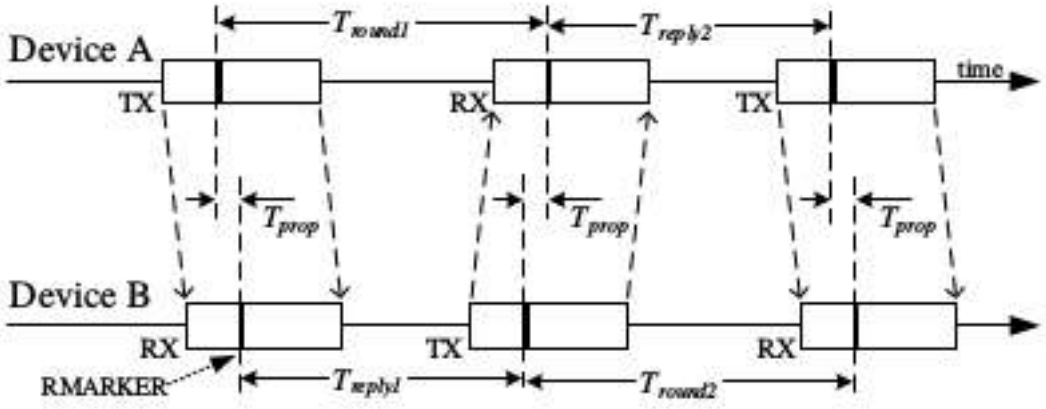

Figure 5.6: Double Sided Two Way Ranging [17]

$$T_{prop} = \frac{timeRound1 \cdot timeRound2 - timeReply1 \cdot timeReply2}{timeRound1 + timeRound2 + timeReply1 + timeReply2} \tag{5.3}$$

As stated earlier the resulting error in DSTWR gets reduced. In Equation 5.4 [17], the error calculation in DSTWR can be seen. Here, the clock in the anchor runs at k_A times the desired frequency and the clock in the beacon runs at k_B times the desired frequency. Both k_A and k_B are close to 1 [17].

$$error = (1 - \frac{k_B + k_A}{2}) \cdot T_{prop} \tag{5.4}$$

It can be seen, that in difference to the SSTWR, the resulting error is independent of the reply time. Furthermore even with the worst case clock error specification stated in the user manual and directions that make their combined error additive the k values might both be 0.99998 and 1.00002 [17]. So for a time-of-flight of 333 nanoseconds, which is 100 meter in range, the resulting error is 6.7 picoseconds which is approximately 2.2 millimeter. This is a non significant error resulting from clock offset, as the determination of arrival time of the frame is actually more significant [17].
With a clearly reduced clock offset error the double sided two way ranging algorithm seems suited for ranging. Thus this algorithm is the one implemented over the course of this thesis.

Asynchronous vs Synchronous

Further it must be decided, if the chosen algorithm is implemented in a synchronous or asynchronous way.
The synchronous approach requires the reply times of each module to be the same. It can be difficult to achieve a situation, where the reply times at every device are the same, because the calculations required at each device may not be the same. For example, the final message from beacon to anchor will need to embed the created time stamps into the frame, so that the anchor can calculate the time-of-flight. Because symmetric reply times are required, all reply times need to be the longest reply time. When the response delays are flexible, the exchange can be faster.
If symmetric delay times are required, the whole round trip exchange will need to be expanded to accommodate this [17].

To calculate a position out of single ranging multilateration can be used. This requires a combination of multiple ranging distances. Therefore a module has to range to multiple beacons.

For the synchronous and asynchronous approach the needed number of messages to range from an anchor to n beacons differ largely in quantity.
For the asynchronous approach one anchor device sends a frame to n beacons. Each beacon responds with a packet to this anchor in successive responses. The anchor closes off the round with a final frame. Each beacon can now calculate its distance from the anchor after a sequence of just n+2 messages. If the anchor had used the synchronous approach it would be forced to have the same delay for each beacon interaction and a minimum of 3 messages per beacon would be required. In the asymmetric case the number of packets required is n+2 whereas in the symmetric case it is 3n [17].

Beneficial is the use of a symmetric approach only on devices with low computation power or on low energy use. Instead of multiplication and division used in the asynchronous approach, the calculations of the propagation times in a double sided synchronous approach, shown in equation 5.5 [17], require only simpler mathematical operations.

$$T_{prop} = \frac{timeRound1 \; - \; timeReply2 \; + \; timeRound2 \; - \; timeReply1}{4} \tag{5.5}$$

Therefore power can be saved. At usage the modules had a stable power supply, so there was no need to reduce the energy consumption.

5.6 Implemented Algorithm

Based on the stated drawbacks of the synchronous approach, an asynchronous approach was implemented.

Advantages	Disadvantages
Reply times need not to be the same - flexibility	mult. and div. operations are required
error is minimized	

The implemented asynchronous double sided two way ranging algorithm offers a great flexibility in software design, whereas the result error still gets minimized. Drawbacks are the usage of performance intensive operations, especially on low performance and low energy devices.

The implemented algorithm is shown in figure 5.7.

Sending the last data frame extends the classic double sided two way ranging algorithm from figure 5.6. To minimize the data payload in each sent frame, the calculated time data at the beacon side is transmitted in an extra data frame to the anchor. This last frame does not interfere with the classic algorithm, but allows for better test result handling at anchor-side and easier testing. In result, only the anchor knows the distance between the modules, but this is sufficient for the quality evaluation of the ranging.

Ranging Procedure

This algorithm is pseudo programmatically implemented in listing 5.1.

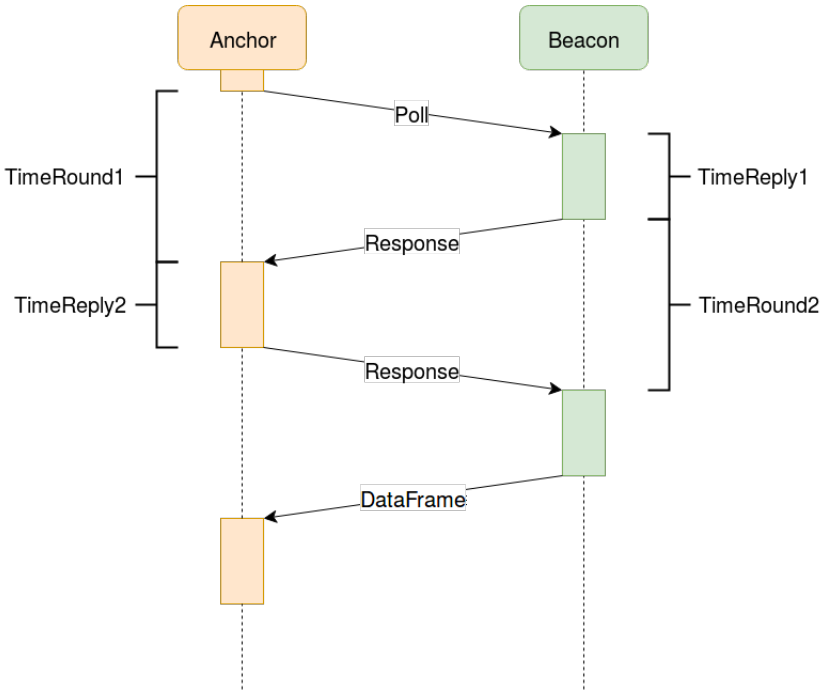

Figure 5.7: Ranging Algorithm

Every transmit and receive triggers an interrupt at the microcontroller and creates a time stamp or starts the sending of a response. At start the anchor transmits a ranging poll to the beacon. The beacon receives this poll and sends a response back to the anchor. Now the anchor receives the response frame and also transmits a response to the beacon. At this point each module has three unique time stamps. With the help of these time stamps the round trip time and reply time can be calculated on each module and the extra frame can be send to the anchor.
Now it is possible to calculate the propagation time from all calculated time

Listing 5.1: Pseudocode of the implemented Ranging Algorithm

```
anchor.sendPoll()
beacon.sendResponse()
anchor.sendResponse()
beacon.sendDataFrame()
anchor.calculateDistance()
```

values at anchor side using equation 5.3. The resulting propagation time is converted to an adequate distance by equation 2.2.

Calculation Accuracy

Because the time stamps consist of 40-bit values, 64-bit integers were used to store them programmatically. By using integer-values no absorption or elimination effects can occur, unlike for addition operations on floating point values [36]. So the use of integers for storing time stamps and calculating differences is favourable here.
To obtain the resulting propagation time, as in equation 5.3, fractions are needed. For this purpose double values were used over integers to store the propagation time, because floating point values can be saved. For multiplication and division operations on double values no negative effects influencing the calculation accuracy exist [23]. Therefore an accurate propagation time can be computed free from error.

By choosing an appropriate algorithm and configuring the module, the implementation aims to create a flexible and robust environment for reducing the effects of disturbing factors. This enables the measurement of accurate distance values. The experimental setup and the evaluation of the experiments is described in the next chapter.

6 Experimental Setup and Evaluation

To evaluate the usefulness and quality of distance values yielded by an ultra-wideband ranging, several experiments have been conducted.
Many interdependend variables like used frequency and multipath effects influence the ranging in unpredictable ways. For this reason each experiment has been designed to evaluate the impact of a single variable on the yielded result values. Influences from other sources have been tried to be kept at a minimum.
While ranging the modules have been fixed in a suitable ranging environment with a constant distance or a constant distance interval between them.
For the distance measurement in each experiment to be representative at least 300 measurements were taken. Also the experiments have been carried out outside the busy times of the faculty and over weekends to reduce noise created by radio frequency interference. Experiments regarding the following topics have been conducted: error over distance, frequency interferences, multipath effects and ranging in motion with and without multipath effects.

6.1 Distance-Error-Correlation

To start the evaluation the ranging results on constant distances were measured. Thence 11 test series were taken on distances from 0 to 5 meters in steps of 50 centimeters. The setup for the measurement at two meters can be seen in figure 6.1.

With the help of the received values it is possible to see how accurate the ranging results are and to calculate a general error.
This experiment sets a baseline for further experiments.

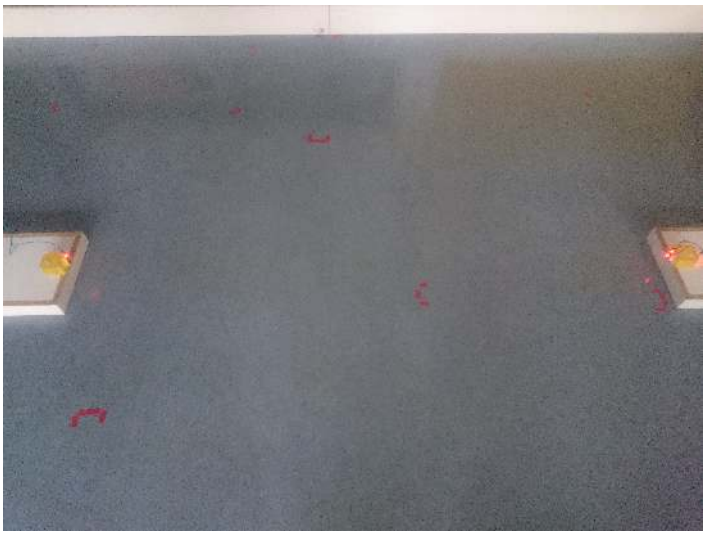

Figure 6.1: Ranging at 2m

In figure 6.2 the received result values are shown. The x-axis shows the real distance between the modules as measurement steps and the y-axis represents the distance values yielded by the ranging.

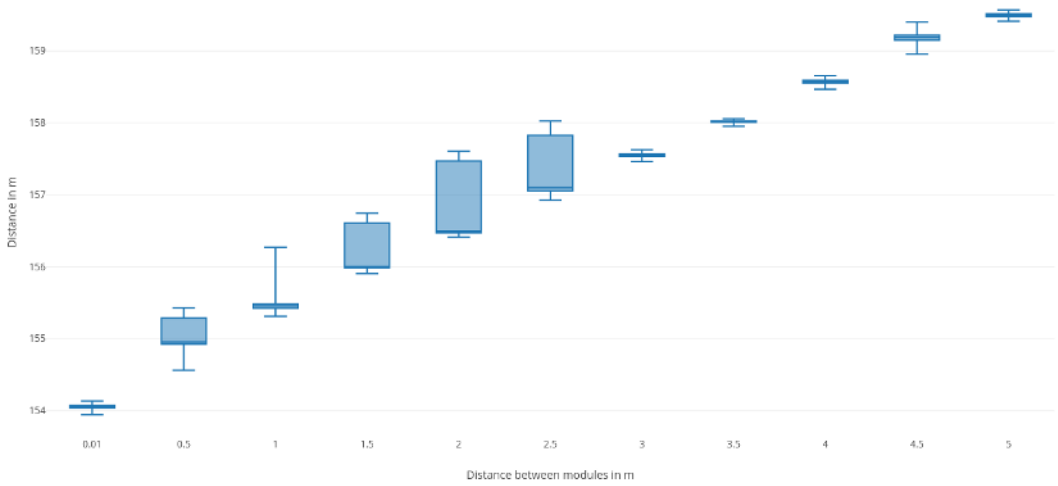

Figure 6.2: Ranging Test Values

Based on the box plots the distribution of distance values on every measurement-step can be seen. Yielded values at measurement-steps above 2.5 meters and at zero meters lie closely together, where as the distribution at steps 0.5 meters to 2.5 meters is much wider.
This is visible in the standard deviation plot shown in figure 6.3. For the wider distributed measurement steps mentioned above deviation values of almost 47 centimeters were measured.

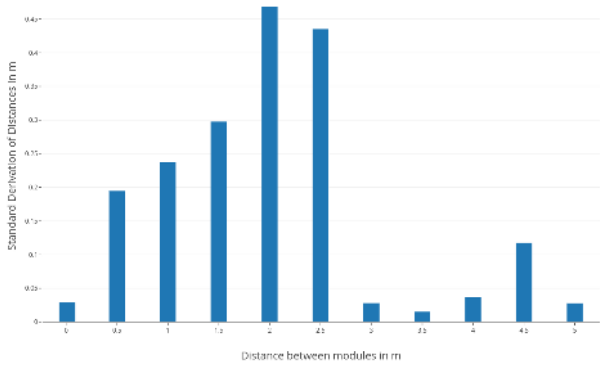

Figure 6.3: Standard Derivation of Distance Values

Why are the distributions for 0.5 meters to 2.5 meters so different from the other measurement steps?
Closer inspection of these yielded range values shows a sudden offset of up to 1 meter added to the values after some time in the ranging. Thus it can be assumed that something influenced the ranging at this point.
No external influences were recognized during the ranging, so internal influences seem to be the cause of this error. After finishing the ranging, the modules were significantly heated. Therefore it is probably related to the increasing module temperature described in 4.2.4. The heat offset at measurement step 1.5 meters is shown in figure 6.4. Similar offset behaviour can be observed at measurement steps 0.5 to 2.5 meters.

Because the heat of the modules is not considered in this thesis and a clear offset is visible, the erroneous measurements can be filtered out. Only the values, that are not affected by heat, are further considered. So an adjusted graph can be created. The adjusted box plot, shown in figure 6.5, now has a significant narrower distribution at the above mentioned measurement steps.

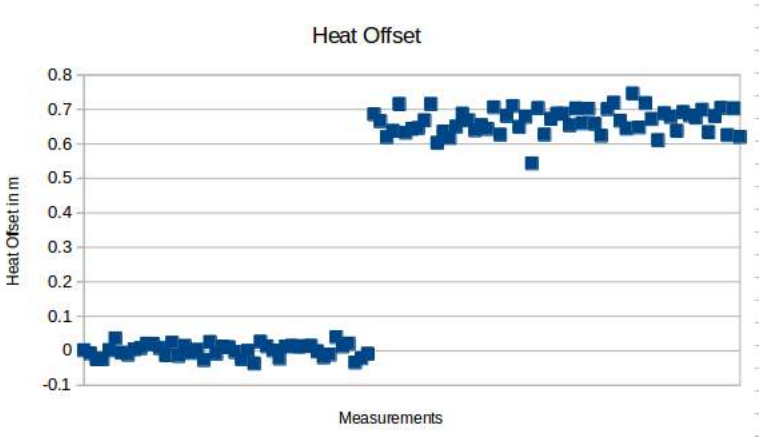

Figure 6.4: Measured Offset at Measurement Step 1.5m

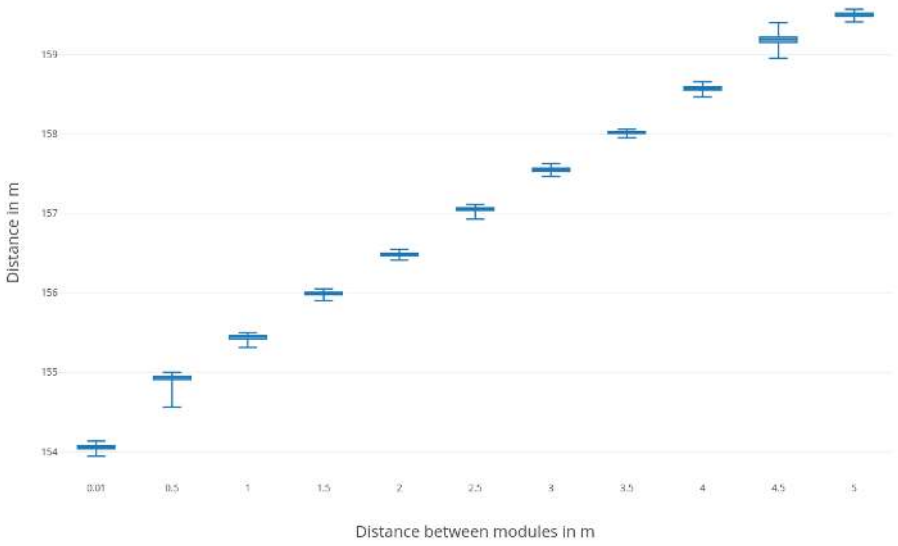

Figure 6.5: Adjusted Ranging Values

But there are critical problems at value range of the yielded result values. All measured values are constantly to high. Instead of the real distance, values over 154 meters were measured.
Out of the adjusted range values a linear characteristic can be derived. Therefore a constant internal fault and thus an error offset, like Zug [48] stated, can be concluded as the reason for the huge distances.
So to remove the error offset, linear regression with squared mean error was

conducted on the adjusted average values. Now it is possible to fit a straight line to the average values yielded by the experiment. This can be seen in figure 6.6.

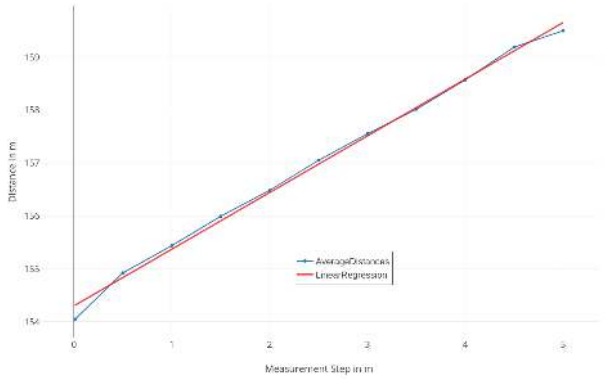

Figure 6.6: Linear Regression on Ranging Values

Based on the fitted line the before mentioned error offset can be determined. The added value in the linear function formula 6.1 is the fitted error offset.

$$f(x) = 1.07 \cdot x + 154.298 \tag{6.1}$$

With a calculated error offset of 154.298 meters the averages of the yielded distance values can be normalized as shown in figure 6.7.

The average values seem to fit the real distances well. They lie within a range of up to 30 centimeters from the real distance. Only the value at measurement-step 4.5 meter differs with a range of 40 centimeters. The adjusted standard deviation plot in figure 6.8 now shows a deviation of the yielded values of under 6 centimeters at every measurement step except 4.5 meters. Step 4.5 meters clearly stands out with almost 12 centimeters of deviation. The yielded values here contain sporadic outlying values. This seems to be caused by some unobserved environmental factors influencing the ranging at this step.

To compensate for outlying values and to get an insight on the number of values close to the average values, confidence intervals with a confidence of 95 percent were calculated.

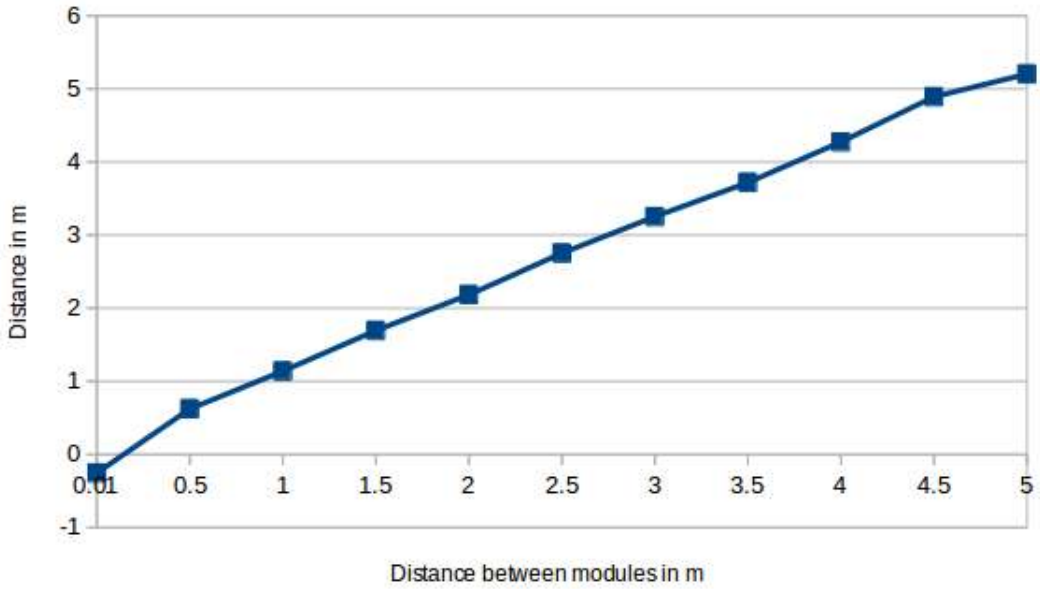

Figure 6.7: Normalized Distance Values

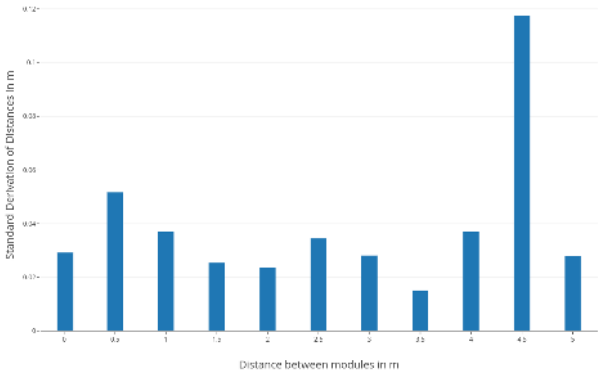

Figure 6.8: Adjusted Standard Deviation

These intervals can be seen in table 6.1. Here, the 2.5% and 97.5% quantile of the confidence interval on every measurement step in meter is shown.

95 percent of the yielded values lie within those boundaries. The calculated confidence intervals at measurement step 0.5 to 5 meters lie above the real distances. Except for measurement step 4.5 and 0.01 meters, the confidence

Table 6.1: Confidence Intervals for Measurement Steps

measurementStep	0.01	0.5	1	1.5	2	2.5	3	3.5	4	4.5	5
2.5% quantile	-0.311	0.522	1.066	1.644	2.137	2.685	3.197	3.6897	4.202	4.774	5.147
97.5% quantile	-0.197	0.725	1.211	1.743	2.23	2.82	3.307	3.749	4.347	4.997	5.256

intervals lie within a similar feasible value range of 20 to 30 centimeters from the real value.
The upper and lower interval boundary at measurement step 4.5 meters is significantly higher. Here an error of 27 to 50 centimeters from the real value is measured. This supports the assumption of unobserved errors during ranging at 4.5 meters, that was discovered through the standard deviation at this measurement step.
The confidence interval at measurement step 0.01 meters is within a feasible value range of 20 to 30 centimeters from the real distance. But here the boundary values are below the real distance and thus negative. This is caused by removing the error offset with the help of a linear regression earlier in this evaluation. Therefore a measured distance gap of up to 1 meter between steps 0.01 and 0.5 meters is given, which must be kept in mind when applying a ranging.

Even though the measured values do not reach the accuracy stated by Michler et al. [35], the yielded values just meet the established requirements from section 1.2. Thus ranging is fundamentally possible, if an adequate security zone is drawn around the module to compensate for the deviating values. Here especially the mentioned distance gap and the existence of negative values must be considered in a ranging application.

For further measurements and experiments the above mentioned results need to be kept in mind. Therefore further experiments on constant distances were conducted above 0.5 meters. Also the deviation of the yielded distance values from the real distances are integrated in further experimental structures and the corresponding evaluation of these experiments.

6.2 Frequency Interferences

To evaluate the impact of frequency interferences on the yielded ranging results several experiments were carried out. Here measurements on every supported frequency channel from 1 to 7 at a constant distance were taken.
The experimental ranging set-up mirrored the setup already used in other experiments shown in figure 6.1. The results yielded by this tests give insight into to robustness of the ranging and can be used to optimize the ranging.

In figure 6.9 the result of the measurements can be seen.

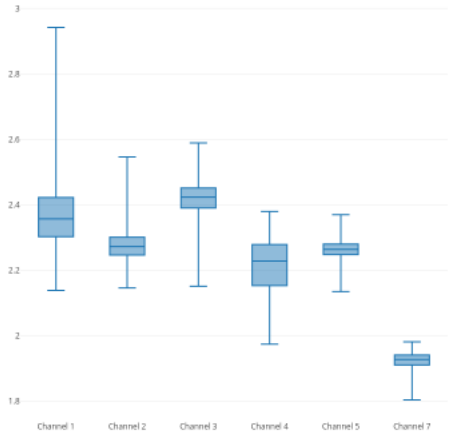

Figure 6.9: Distances on different Channels

On the x-axis the different channels are shown and on the y-axis the corresponding distance values. By looking at the box plots of the yielded values huge differences in value range can be seen. Especially the values on channel 7 are significantly smaller than the other values. With a difference in mean value of almost 30 cm in comparison to the next smallest mean value channel 7 is really standing out. Also on channel 7 the maximal range from smallest to highest distance value is the minimum of all tested channels.
This is correlated with the standard deviation which can be seen in figure 6.10. Here channel 7 is the best performer, too. With a standard deviation of 2.6 centimeters channel 7 delivers the best results.

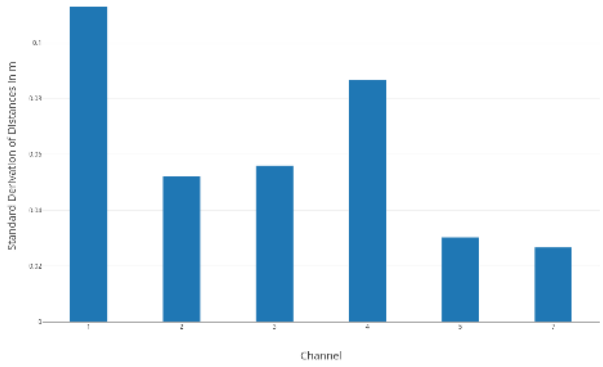

Figure 6.10: Standard Deviation of Distance Values related to Channel

How does channel 7 perform so well as opposed to the other channels?
As seen in figure 3.1 channel 7 has the second largest frequency bandwidth after channel 4. The bandwidth is 216 percent broader than most other channels channels. Therefore the probability to transceive on a frequency already in use is lowered.
The channel spectra in figure 6.11 taken from the data sheet[18], provide even more insight into the channel characteristics. Here, the power level of transmission on each frequency in the selected channel can be seen. It is obsevable, that additionally to the extended bandwidths, channel 7 and 4 transceive with a higher power level on a wider range of usable frequencies. So the average power level of a transmissions in these channels is higher than in all other channels. This enables a more robust transmission.

Additional external influences, that need to be considered are overlapping frequencies from other devices. Especially with the overlapping 5 GHz WLAN channel, there should be noticeable impact in yielded values.

The free usage of 5 GHz WLAN is limited to two sections, one from 5.15 to 5.35 GHz and one from 5.47 to 5.725 GHz [13].
With a lower frequency boundary of 5.408 GHz, channel 7 utilizes bandwidths overlapping with just one section of the 5 GHz WLAN. Also WLAN on this frequency is a newer technology, so the number of users is still relatively small. This limits the impact of WLAN on this channel.

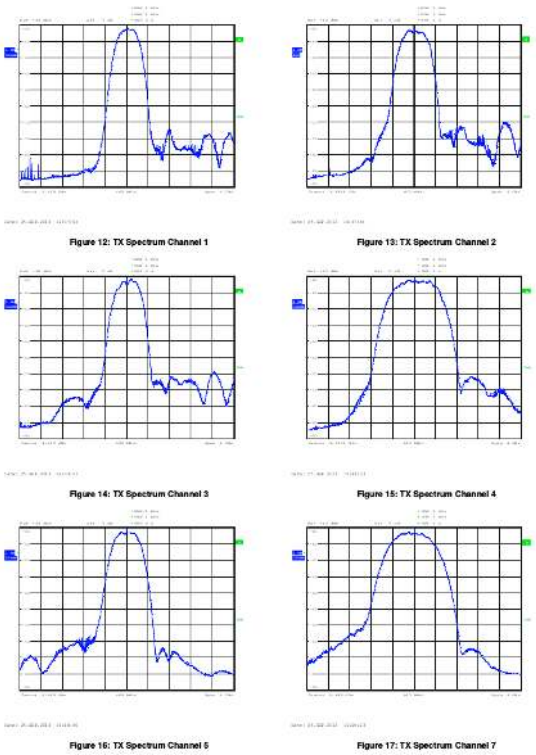

Figure 6.11: Signal Strength-Frequency-Correlation for Channels[18]

Furthermore the precipitation radar used in the EU utilizes bandwidths from 5.58 to 5.66 GHz [8]. For devices using the 5 GHz WLAN not to interfere in radar measurements, an obligatory Dynamic Frequency Selection (DFS) [16] standardized by the EU [26] has to be implemented. This means as soon as a device detects radar frequencies, a switch in frequency will take place to avoid co-channel operations with the radar. Thus the impact of 5 GHz WLAN on channel 7 gets further reduced, by utilizing less frequencies overlapping with channel 7.

In the experiment conducted, channel 7 stands out in terms of ranging quality. This is caused by the larger bandwidth of this channel, as well as by specific frequency interferences during this experiment.
This can change with a change in environment, but with the possibility to switch the used channel, the applicability of the ranging increases. Because the bandwidth and center frequency can be configured to avoid dominant frequencies, the ranging can be used with a large variety of influencing frequencies and thus in a large variety of areas and applications. Though a configuration

at application setup is necessary.
Nevertheless best values can be achieved, if interfering frequencies are minimal.

6.3 Multipath

Objects between ranging modules can influence the yielded result values. To evaluate the impact a single object in the line of sight has, the result values of a non line-of-sight measurement were compared with the values yielded by a line-of-sight measurement. Therefore a 25x15x20 centimeter box made of aluminium was placed in between the modules used for the ranging. Because of it's high conductivity aluminium is used to block the propagation of radio waves [44]. So the line of sight between the modules is obstructed.
Figure 6.12 shows the non line-of-sight measurement setup and in figure 6.1 the line-of-sight setup can be seen. The modules were 1.5 meters apart for the experiments.
With the help of the results information about the applicability of ranging in a non line-of-sight environment can be gathered.

Figure 6.12: NLOS-Setup

The comparison of distance values between a non line-of-sight(NLOS) and a line-of-sight measurement is shown in figure 6.13. Both measurements were taken using the same distance between the modules.

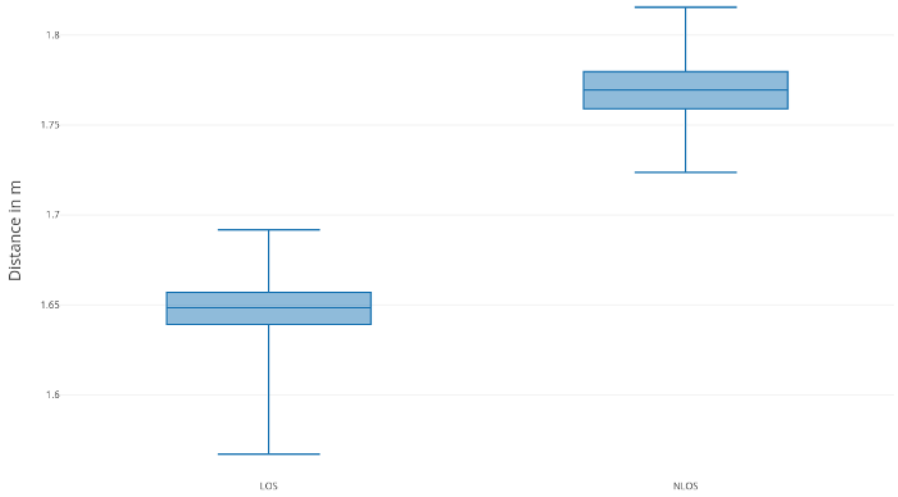

Figure 6.13: Comparison NLOS-LOS

Noticeable here is that the box plots generated out of the yielded result values are non-overlapping. Their medians have a difference in value of about 12 centimeters.
The correlated mean values of the measurements mirror the above stated difference. This can be seen in figure 6.14.

It is clearly to see, that placing an object in the ranging line-of-sight of the modules inhibits the propagation of the radio waves. Whether the radio waves get reflected from the object or a diffraction happens around the the object, the elapsed propagation time gets prolonged as Lee and Scholtz [30] stated.
In the measurement an incorrect average distance with an offset of over 10 centimeters was measured. This is even more concerning in relation to the size of the object that was used to block the radio waves. With 20cm x 30cm x 20cm a small blocking object was used. If the size of the used object increases the path of the radio waves around the object will increase as well. This leads to even larger offsets in yielded distance values.

The above mentioned multipath characteristics limit the applicability of the ranging to open areas without many objects. The error in yielded ranging values increases with number and size of objects in the application area.

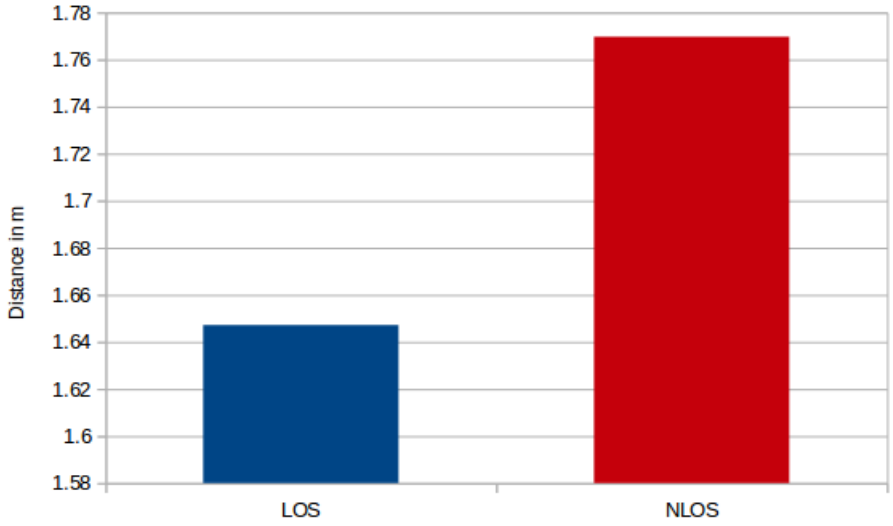

Figure 6.14: Mean Values LOS vs NLOS

6.4 Ranging in Motion

A ranging is mostly useful in applications, only if the measured distance is changing. That includes drones, logistic robots, mobile robots and many more. To test the ranging modules in motion, experiments were conducted. One module was mounted on a rotating circular plane and another was fixed stationary at the edge of the plane. This setup can be seen in figure 6.15.
While rotating about every two seconds the distance between the modules was measured.

In order to state a function, that approximates the distance over time, the position of the module on the circular path can be used as an approach. Regarding the unit circle, this position can be calculated with the sine and the cosine of the angle. Furthermore the distance is measured from the border, not from the center, so the radius, which is 1 for the unit circle, must be added to the sine function. This can be seen in figure 6.16. The position coordinates are computable with the following equations.

$$x = sin(\alpha) + 1 \tag{6.2}$$

$$y = cos(\alpha) \tag{6.3}$$

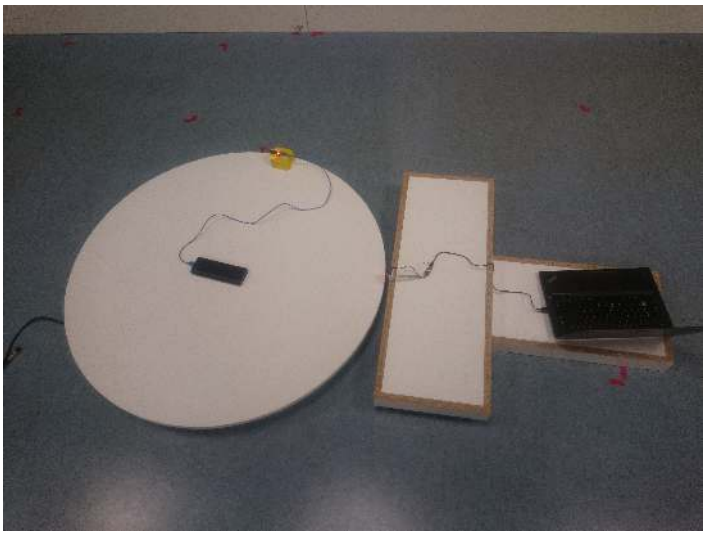

Figure 6.15: Setup Ranging in Motion

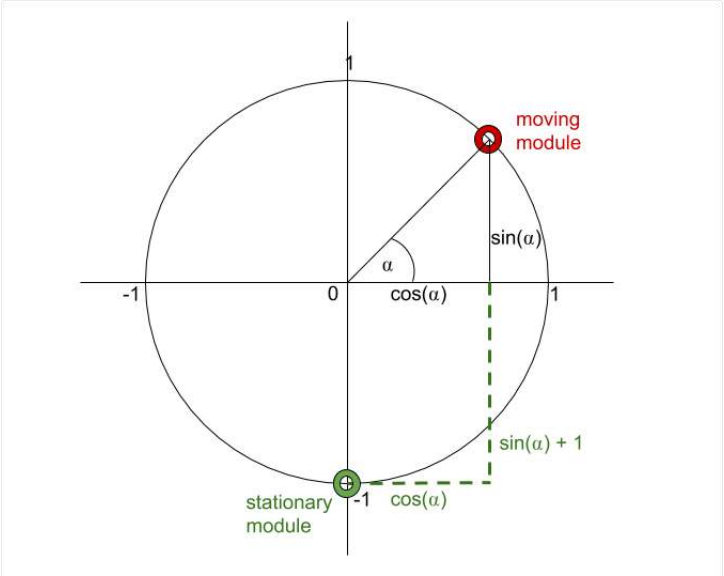

Figure 6.16: Experimental Sketch at Unit Circle

The distance r to the origin is $\sqrt{x^2 + y^2}$. With formulas from 6.2 and 6.3 the distance between the modules is calculated with equation 6.4.

$$r = \sqrt{(sin(\alpha) + 1)^2 + cos(\alpha)^2} \tag{6.4}$$

Pythagoras ($sin(\alpha)^2 + cos(\alpha)^2 = 1$) reduces the formula.

$$r = \sqrt{2} \cdot \sqrt{sin(\alpha)^2 + 1} \tag{6.5}$$

Equation 6.5 is the basis for the next steps. With the angular velocity, $\omega = 2 \cdot \pi \cdot f$, the angle is calculated as in equation 6.6.

$$\alpha = 2 \cdot \pi \cdot f \cdot t + \phi \tag{6.6}$$

Due to the fact the experiment is not constructed on the unit circle, the amplitude must be multiplied to the sine function in equation 6.5. Moreover the angle in this equation is replaced by 6.6. This leads to the distance formula shown in 6.7.

$$d = \sqrt{2} \cdot \sqrt{\hat{r} \cdot (sin(2 \cdot \pi \cdot f \cdot t + \phi)^2 + 1)} \tag{6.7}$$

With the help of an optimizing algorithm the parameters $\hat{r}, \phi, f$ are adjusted.

In figure 6.17 the comparison of the original values and the approximation can be seen.

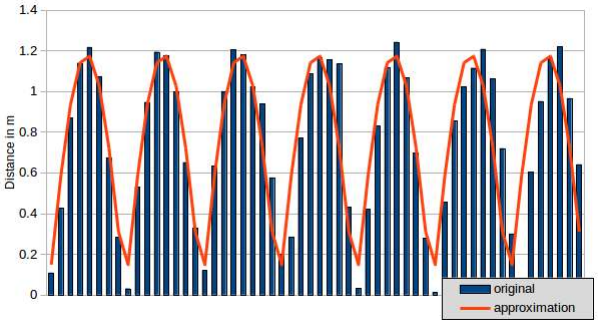

Figure 6.17: Ranging in Motion

The oscillating distance implies the circular movement of the module. This is clearly visible in the measurement values.

Further the average deviation of the yielded values from the approximation was computed. The average error from the approximation is 12 cm and the

standard deviation of this error is about 12 cm as well. These values lie within the range of the confidence interval calculated and shown in table 6.1.

Outlying deviation values occur especially with decreasing sinus function.
This can be explained by the changing orientation of the ranging module during the experiment.
With falling sine function, the non-stationary ranging module is located in the horizontally polarized plane of the antenna.
That means the angle between the line of sight of the modules and the propagation direction of the radio wave can be up to 90 degrees. This decreases the power level of the transmission and so enables erroneous measurements as described in 3.1.
Additionally with falling sine function the board, on which the ranging module was soldered, is in direct line of sight between the ranging modules and blocks a portion of the transmitted signal, which leads to a longer propagation time through multipath effects as evaluated in 6.3.

The use of the ranging in motion is fundamentally possible as the average error of the measurement values is low.
However the changing orientation of the ranging modules during motion has a significantly impact on the measured distances, which can lead to false results. Therefore when used on mobile robots, particular attention must be paid to the orientation and attachment of the ranging modules.

6.5 Ranging in Motion & Multipath

Mobile robots used in real life applications are able to drive past and behind obstacles. Here multiple influences get combined and can lead to heavy disturbances in ranging.
To analyze these disturbances, an obstacle was used to modify the earlier setup. Figure 6.18 shows the modified setup.

The basic setup was just slightly modified so the same functional characteristics used in the earlier motion experiment can be applied. However a difference in result is expected.

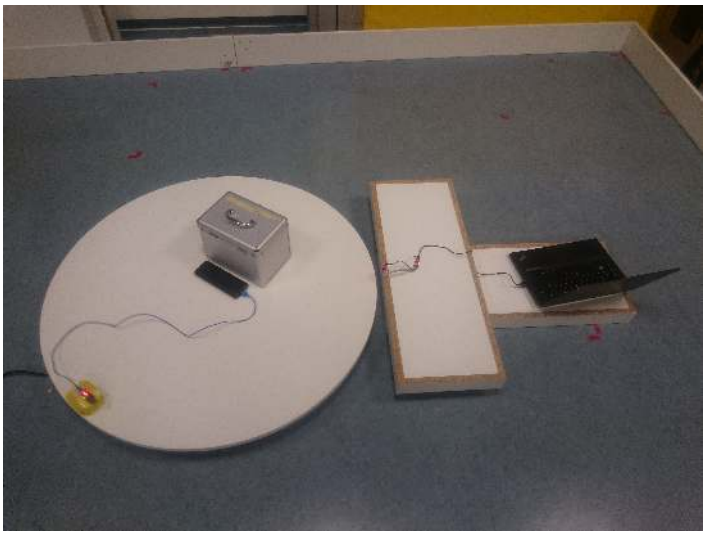

Figure 6.18: Setup Ranging in Motion & Multipath

Figure 6.19 shows the values yielded by the non line of sight measurement.

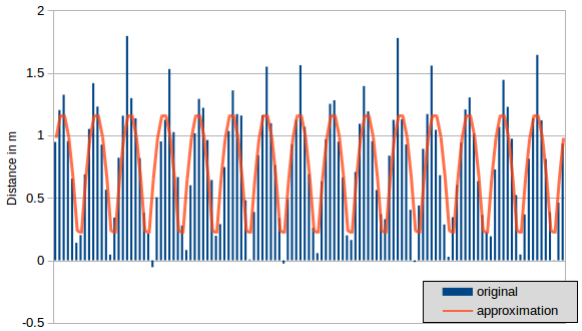

Figure 6.19: Ranging in Motion & Multipath

It can be seen that the used object influences the ranging significantly. The average error of the yielded values from the approximation increases from 12 cm without the object to 17 cm with it. Also the standard deviation of the error is higher with about 15 cm. A direct comparison of both experiments in motion is given in table 6.2.

The width of the object used is 20 percent of the maximal distance between the ranging modules. This influences the propagation time due to severe multipath effects.

Table 6.2: Comparison Ranging in Motion & Multipath

	Motion	Motion + Multipath
Average Error	12.1 cm	17.8 cm
Standard Deviation	12.3 cm	15.1 cm

The object has the strongest influence on the ranging, when it is in a direct line of sight between the modules.
Once the object moves out of the line of sight, the measured values normalize and match the values in the previous experiment without the blocking object.

Since the orientation and attachment of the modules has not changed compared to the previous experiment, they also have an influence on the measurement results.
This results in the interference of multipath effects by the object as well as by the orientation of the antenna itself.
The resulting error is therefore massively increased and leads to a maximum deviation from the approximation of 0.7 meters.
For smaller or more distant blocking objects, the occurring multipath effects are lower.

After all experiments have been conducted, a summarized statement about ranging with ultra wideband can be made. A conclusion is given in the next chapter.

7 Conclusion

In summary, the single distance measurements with ultra wideband are feasible. Here *DecaWave* DWM1000 modules were utilized to measure the time of flight and calculate an adequate distance.
Indoor ranging tests up to a distance of 5 meters provide useless measured results over 154 meters. After a suitable filtering and error compensation, a mean error from the real distance of less than 30 centimeters could be achieved. For other scenarios, besides the one used, this might not be possible. The standard deviation of the measured values is below 6 centimeters. The requirements for a use in a quadcopter swarm of a mean error below 30 centimeters and a standard deviation of less than 15 centimeters, stated in section 1.2, are fulfilled.

In order to minimize or completely avoid external influences on the ranging accuracy due to frequency interferences, the used frequency band from 3.5 GHz to 7.5 GHz is selectable through predetermined channels. Results in section 6.2 show differences in distance of up to 50 centimeters depending on the used transmit channel.
Furthermore multipath effects by blocking objects have a big impact on the accuracy of the ranging. For the used experimental setup, differences of up to 15 centimeters between a line of sight and a non line of sight measurement are observable. This influences the applicability of the ranging. It is not suitable, if there are multiple blocking objects between the ranging modules. By reducing the effects of external influences, measurement robustness can be achieved.

Orientation changes of the ranging modules during motion are causing inaccurate measured values and therefore have to be considered as well. A suitable implementation on the robot can minimize these effects, but a poor implementation on mobile robots, can lead to inaccuracies and multipath effects with the robot itself. Another problem is the increase of the module temperature during ranging. It significantly influences the quality of the yielded measurements. For the use in a quadcopter swarm scenario with a continuous cooling

air stream, it is negligible, but it must be considered for the implementation in other applications and other mobile robots.

If several errors accumulate to a single high error, the measured distances can become very bad to unusable.

In future work, persistent inaccuracies can be minimized and the ranging, as well as its application, can be improved. This is further described below.

To reduce existing inaccuracies suitable filters can be used on the yielded values and thus improve the achieved accuracy of the ranging.

The evaluation in this thesis is limited due to a controlled environment. To further evaluate the applicability, field tests must be performed. For real application scenarios, the ranging can be integrated in robots and the performance in a multilateration localization application can be estimated. Here the accuracy of a positioning solution and possible interferences by using more than two ranging modules can be evaluated. Also experiments on the maximum usable distance of the ranging can be conducted. Further the relation of different power management settings of the ranging modules to yielded measurement quality, can be evaluated and an optimal power managment setting for different applications can be found. Another existing problem is the temperature increase of the modules. Hence the effect of heat on the yielded measurement values can be analyzed in further experiments.

The future application on mobile robots is subject to procedural limitations, due to multipath effects and frequency interferences. But with continuous improvement of accuracy and robustness, it can be used for localization in GPS-denied environments.

Bibliography

[1] Digikey - at86rf233-zur. https://www.digikey.com/product-detail/en/microchip-technology/AT86RF233-ZUR/AT86RF233-ZURCT-ND/3775085. Accessed: 19.01.2019.

[2] Future electronics - decawave dwm1000. https://www.futureelectronics.com/p/wireless-rf--rf-modules-solutions--proprietary/dwm1000-decawave-7090231. Accessed: 19.01.2019.

[3] Migatroncorp - applications of ultrasonic sensors. https://www.migatron.com/ultrasonic-detections-and-control-applications/. Accessed: 04.01.2019.

[4] Optitrack - compare cameras. https://optitrack.com/hardware/compare/. Accessed: 19.01.2019.

[5] Robotshop - ultrasonic range finders. https://www.robotshop.com/en/ultrasonic-range-finders.html. Accessed: 19.01.2019.

[6] Speed of light. https://en.wikipedia.org/wiki/Speed_of_light. Accessed: 21.01.2019.

[7] Ieee standard for local and metropolitan area networks–part 15.4: Low-rate wireless personal area networks (lr-wpans). *IEEE Std 802.15.4-2011 (Revision of IEEE Std 802.15.4-2006)*, pages 1–314, Sep. 2011.

[8] Wlan-frequencies and weather radar. https://wiki.freifunk-franken.de/w/WLAN_Frequenzen#UNII-2_Extended_.285470_-_5725.29, January 2018. Accessed: 17.01.2019.

[9] Daron Acemoglu and Pascual Restrepo. Robots and jobs: Evidence from us labor markets. 2017.

[10] Salih Alcay and Cemal Ozer Yigit. Network based performance of gps-only and combined gps/glonass positioning under different sky view conditions. *Acta Geodaetica et Geophysica*, 52(3):345–356, Sep 2017.

[11] Bitcraze. Bitcraze libdw1000 - driver for dw1000. `https://github.com/bitcraze/libdw1000`.

[12] Alexandre Greff Buaes. A low cost one-camera optical tracking system for indoor wide-area augmented and virtual reality environments. 2006.

[13] Bundesnetzagentur. Allgemeinzuteilung von frequenzen in den bereichen 5150 mhz-5350 mhz und 5470 mhz - 5725 mhz für funkanwendungen zur breitbandigen datenübertragung, was/wlan, 2018.

[14] Roberta Cardinali, Luca De Nardis, M-G Di Benedetto, and Pierfrancesco Lombardo. Uwb ranging accuracy in high-and low-data-rate applications. *IEEE Transactions on Microwave Theory and Techniques*, 54(4):1865–1875, 2006.

[15] J David N Cheeke. *Fundamentals and applications of ultrasonic waves*. CRC press, 2016.

[16] Sunghyun Choi, Stefan Mangold, and Amjad Soomro. Dynamic frequency selection scheme for ieee 802.11 wlans, April 17 2007. US Patent 7,206,840.

[17] DecaWave Ltd. *DW1000 User Manual*, 6 2015. Revision 2.05.

[18] DecaWave Ltd. *DW1000 Datasheet*, 3 2016. Revision 2.09.

[19] DecaWave Ltd. *DWM1000 Datasheet*, 6 2016. Revision V1.4.

[20] Francisco Domingo-Perez, Jose Luis Lazaro-Galilea, Andreas Wieser, Ernesto Martin-Gorostiza, David Salido-Monzu, and Alvaro de la Llana. Sensor placement determination for range-difference positioning using evolutionary multi-objective optimization. *Expert Systems with Applications*, 47:95 – 105, 2016.

[21] Eiman Elnahrawy, Xiaoyan Li, and Richard P Martin. The limits of localization using signal strength: A comparative study. In *Sensor and Ad Hoc Communications and Networks, 2004. IEEE SECON 2004. 2004 First Annual IEEE Communications Society Conference on*, pages 406–414. IEEE, 2004.

[22] Qing Fu and Guenther Retscher. Active rfid trilateration and location fingerprinting based on rssi for pedestrian navigation. *The Journal of Navigation*, 62(2):323–340, 2009.

[23] David Goldberg. What every computer scientist should know about floating-point arithmetic. *ACM Computing Surveys (CSUR)*, 23(1):5–48, 1991.

[24] Fredrik Gustafsson and Fredrik Gunnarsson. Positioning using time-difference of arrival measurements. In *ICASSP (6)*, pages 553–556. Citeseer, 2003.

[25] Kelly D Hawkes and Jeffrey L Koehler. Time difference of arrival measurement system, March 13 2001. US Patent 6,201,499.

[26] European Telecommunications Standards Institute. Etsi en 301 893 - 5 ghz rlan; harmonised standard covering the essential requirements of article 3.2 of directive 2014/53/eu, 5 2017.

[27] Zhang T Jin B, Xu X. Robust time-difference-of-arrival (tdoa) localization using weighted least squares with cone tangent plane constraint.

[28] Kamol Kaemarungsi. Distribution of wlan received signal strength indication for indoor location determination. In *Wireless Pervasive Computing, 2006 1st International Symposium on*, pages 6–pp. IEEE, 2006.

[29] Rasool Khadem, Clement C Yeh, Mohammad Sadeghi-Tehrani, Michael R Bax, Jeremy A Johnson, Jacqueline Nerney Welch, Eric P Wilkinson, and Ramin Shahidi. Comparative tracking error analysis of five different optical tracking systems. *Computer Aided Surgery*, 5(2):98–107, 2000.

[30] Joon-Yong Lee and Robert A Scholtz. Ranging in a dense multipath environment using an uwb radio link. *IEEE Journal on Selected Areas in Communications*, 20(9):1677–1683, 2002.

[31] Chang-Beom Lim, Sung-Hun Kang, Hyun-Hun Cho, Sin-Woo Park, and Joon-Goo Park. An enhanced indoor localization algorithm based on ieee 802.11 wlan using rssi and multiple parameters. In *Systems and Networks Communications (ICSNC), 2010 Fifth International Conference on*, pages 238–242. IEEE, 2010.

[32] Sebastian Mai. Wireless ranging in swarm robotics. 2015/2016.

[33] Rainer Mautz. Overview of current indoor positioning systems. *Geodezija ir kartografija*, 35(1):18–22, 2009.

[34] Audiovisuelle Medien. Implementation of a low cost marker based infrared optical tracking system. 2006.

[35] Fabian Michler, Harun Deniz, Fabian Lurz, Robert Weigel, and Alexander Koelpin. Performance analysis of an ultra wideband transceiver for real-time localization. In *2018 48th European Microwave Conference (EuMC)*, pages 1141–1144. IEEE, 2018.

[36] Jean-Michel Muller, Nicolas Brisebarre, Florent De Dinechin, Claude-Pierre Jeannerod, Vincent Lefevre, Guillaume Melquiond, Nathalie Revol, Damien Stehlé, Serge Torres, et al. Handbook of floating-point arithmetic. 2010.

[37] Roger Muncaster. *A-level Physics*. Nelson Thornes, 1993.

[38] R. Paschotta. phase shift method for distance measurements. `https://www.rp-photonics.com/phase_shift_method_for_distance_measurements.html`. Accessed: 17.01.2019.

[39] Ling Pei, Ruizhi Chen, Jingbin Liu, Heidi Kuusniemi, Tomi Tenhunen, and Yuwei Chen. Using inquiry-based bluetooth rssi probability distributions for indoor positioning. *Journal of Global Positioning Systems*, 9(2):122–130, 2010.

[40] Lanxin Qiu, Zhangqin Huang, Shaohua Zhang, Cheng Jing, Hao Li, and Shuyao Li. Multifrequency phase difference of arrival range measurement: principle, implementation, and evaluation. *International Journal of Distributed Sensor Networks*, 11(11):715307, 2015.

[41] William H Strickland and Robert H King. *Characteristics of ultrasonic ranging sensors in an underground environment*. US Department of the Interior, Bureau of Mines, 1993.

[42] Ali Taha and Keith M Chugg. A theoretical study on the effects of interference uwb multiple access impulse radio. In *Signals, Systems and Computers, 2002. Conference Record of the Thirty-Sixth Asilomar Conference on*, volume 1, pages 728–732. IEEE, 2002.

[43] J.R. Taylor. *Introduction To Error Analysis: The Study of Uncertainties in Physical Measurements*. A series of books in physics. University Science Books, 1997.

[44] Christopher J von Klemperer and Denver Maharaj. Composite electromagnetic interference shielding materials for aerospace applications. *Composite Structures*, 91(4):467–472, 2009.

[45] Kamin Whitehouse, Chris Karlof, and David Culler. A practical evaluation of radio signal strength for ranging-based localization. *ACM SIGMOBILE Mobile Computing and Communications Review*, 11(1):41–52, 2007.

[46] Moustafa Youssef. *Indoor Localization*, pages 1004–1010. Springer International Publishing, Cham, 2017.

[47] Li Zhao and Alexander M Haimovich. Performance of ultra-wideband communications in the presence of interference. *IEEE Journal on Selected Areas in Communications*, 20(9):1684–1691, 2002.

[48] S. Zug, A. Dietrich, and J. Kaiser. An architecture for a dependable distributed sensor system. *IEEE Transactions on Instrumentation and Measurement*, 60(2):408–419, Feb 2011.

Declaration of Authorship

I hereby declare that this thesis was created by me and me alone using only the stated sources and tools.

Markus Hempel Magdeburg, January 22, 2019